THE JOURNAL OF COMPARATIVE NEUROLOGY 491:305–319 (2005)

Pretarget Sorting of Retinocollicular Axons in the Mouse

DANIEL T. PLAS,[1] JOSHUA E. LOPEZ,[1] AND MICHAEL C. CRAIR[1,2]*
[1]Department of Neuroscience, Baylor College of Medicine, Houston, Texas 77030
[2]Program in Developmental Biology, Baylor College of Medicine, Houston, Texas 77030

ABSTRACT

ABSTRACT The map of the retina onto the optic tectum is a highly conserved feature of the vertebrate visual system; the mechanism by which this mapping is accomplished during development is a long-standing problem of neurobiology. The early suggestion by Roger Sperry that the map is formed through interactions between retinal ganglion cell axons and target cells within the tectum has gained significant experimental support and widespread acceptance. Nonetheless, reports in a variety of species indicate that some aspects of retinotopic order exist within the optic tract, leading to the suggestion that this "preordering" of retinal axons may play a role in the formation of the mature tectal map. A satisfactory account of pretarget order must provide the mechanism by which such axon order develops. Insofar as this mechanism must ultimately be determined genetically, the mouse suggests itself as the natural species in which to pursue these studies. Quantitative and repeatable methods are required to assess the contribution of candidate genes in mouse models. For these reasons, we have undertaken a quantitative study of the degree of retinotopic order within the optic tract and nerve of wild-type mice both before and after the development of the retinotectal map. Our methods are based on tract tracing using lipophilic dyes, and our results indicate that there is a reestablishment of dorsoventral but not nasotemporal retinal order when the axons pass through the chiasm and that this order is maintained throughout the subsequent tract. Furthermore, this dorsoventral retinotopic order is well established by the day after birth, long before the final target zone is discernible within the tectum. We conclude that pretarget sorting of axons according to origin along the dorsoventral axis of the retina is both spatially and chronologically appropriate to contribute to the formation of the retinotectal map, and we suggest that these methods be used to search for the molecular basis of such order by using available mouse genetic models. J. Comp. Neurol. 491:305–319, 2005.

Indexing terms: development; chemoaffinity; retinotectal; superior colliculus; vision; retinotopy

The pattern of topographic projection of the retina onto the optic tectum is shared by all vertebrates. This map has served as the main model of neural specificity, exhibiting the ability of a large number of projecting neurons to connect via their axons to a distant target in such a way as to reproduce the spatial layout of the projecting structure. Details of the retinotectal map have been characterized in fish, amphibians, birds, reptiles, and mammals, all of which are found to share many essential features. Nonetheless, after more than half a century of research, we still lack a full account of the developmental events and mechanisms by which this, or any other, retinotopic map is established.

Following the work of Roger Sperry (1963), most investigators have attempted to explain the development of retinotectal and other neural maps according to a chemoaffinity model. In this scheme, projecting neurons achieve their connectional specificity by virtue of chemical signatures borne on their navigating axons. Although this is often understood to be a principle that operates solely

Grant sponsor: National Institutes of Health; Grant number: R01 EY015788; Grant number: R01 MH62639; Grant number: T32 EY07001; Grant sponsor: the Klingenstein Foundation; Grant sponsor: the Merck Foundation; Grant sponsor: the Sloan Foundation; Grant sponsor: the American Heart Association; Grant sponsor: the National Alliance for Research on Schizophrenia and Depression (to M.C.C.); Grant sponsor: Discovery Lab through the National Institutes of Health; Grant number: R25 RR18595 (to J.L.); Grant sponsor: the A+ Challenge (to J.L.).

*Correspondence to: Michael C. Crair, Baylor College of Medicine, One Baylor Plaza, S-603, Houston, TX 77030. E-mail: mcrair@bcm.edu

Received 4 March 2005;Revised 28 April 2005; 3 May 2005

DOI 10.1002/cne.20694

Published online in Wiley InterScience (www.interscience.wiley.com).

within the target tissue, Sperry initially contemplated the possibility that these chemical signatures might be recognized by landmarks en route, which might serve to organize the fiber tracts themselves (Attardi and Sperry, 1963). Sperry later revised his model to include matched chemical gradients between projecting neurons and their targets (Sperry, 1964). It is this form of the "chemoaffinity hypothesis" that today has gained wide assent, with the receptor tyrosine kinase families of Eph receptors and their ephrin ligands having emerged as leading candidates to play the role of chemoaffinity cues.

Despite the current dominance of Sperry's matched gradient chemoaffinity model, several studies have indicated that retinal ganglion cell (RGC) axons do exhibit some features of retinotopic order within the optic tract. It should be stated outright that a robust and precise retinotopy comparable to that within the tectum itself is definitely not discernible in either the optic nerve or optic tract of any species. What has been reported is a partial and approximate order, and this fact has complicated comparison of results obtained in different species, by different workers, and by use of different methods. Anamniotes exhibit the clearest and most extensive preservation of order in the retinal projection. In fish and amphibians, for instance, a considerable degree of retinotopy has been reported throughout the retinofugal projection (Bunt and Horder, 1983). An extensive study using retrograde transport of horseradish peroxidase (HRP) in chicks (Rager et al., 1988) revealed a similar degree of order, with the authors interpreting the repeated reorganization of fibers in the axonal tract as a mechanism to prepare them for the retinotopic innervation of each successive retinal target.

Among mammals the pattern of pretarget order is more variable, and even within the mammals studied, various degrees of "preordering" have been reported. In reviewing the scattered literature on this topic, meaningful comparisons are frequently precluded by the often anecdotal and qualitative descriptions of the phenomena involved. One study addressed the order of retinal axons in the optic nerve of the cat (Horton et al., 1979). This study used retrograde transport of HRP injected into a small region of the lateral geniculate nucleus, resulting in a small cluster of labeled retinal ganglion cells. It was observed that within the optic nerve, the labeled axons diverged widely from one another and thus could not be confined to a retinotopic arrangement. In marsupials, however, there does appear to be rather good preservation of retinotopy even in the optic nerve (Dunlop et al., 2000). A study in rats (Simon and O'Leary, 1991) revealed an almost total loss of retinotopic order as axons reached the chiasm. In general, the conclusion from the literature is that an initial retinotopic order of axons as they exit the eyeball is greatly degraded along the course of the optic nerve, so that virtually no order remains upon reaching the chiasm.

Despite the evidence that retinal axons are more or less randomly distributed in the optic nerve in at least some mammals, it has been noticed that in those same animals dorsal and ventral axons show some degree of segregation after they have passed through the chiasm. This has been reported in the cat (Torrealba et al., 1982), ferret (Walsh and Guillery, 1985), monkey (Naito, 1989), and embryonic rat (Chan and Guillery, 1994). In the embryonic rat, for example, the authors concluded that dorsal and ventral axons become more or less segregated into the mediocaudal and rostrolateral aspects, respectively, of the ascending optic tract. The optic chiasm is well known as a point of axon rearrangement, mediating, for example, the sorting of ipsi- and contralaterally projecting axons. It is thus conceivable that additional mechanisms might exist at the chiasm to reestablish at least some aspects of retinal topography among the retinal axons as they pass through.

It is possible that both presorting mechanisms and within-target interactions are required for the proper formation of the retinotectal map. In this case, the objection that the observed presorting is "too crude" to explain the final precision of the map may be beside the point. Perhaps only a rough pretarget sorting is required in order for within-target interactions to be successful. It has also been suggested that, although some pretarget order is present, at least in some species, this order is coincidental and not a carefully regulated process that is required for map formation. Studies of the cat optic tract have particularly contributed to this view (Walsh et al., 1983). The dorsal retinal ganglion cells of the cat are generated before those in the ventral retina, and it has been suggested that this fact accounts for the observed tendency of dorsal axons to lie on the medial aspect of the tract, with later arriving ventral growing over the surface and thus laterally. This pattern, however, does not preclude the possibility that the postchiasmatic ordering of dorsal and ventral axons is specifically regulated by dorsoventral origin and not merely time of arrival. A careful study of another carnivore, the ferret, has suggested that an active sorting mechanism redistributes dorsal and ventral RGC axons to their own territories within the optic tract after exiting the chiasm (Reese and Baker, 1993).

If the order that has been described in the pretectal tract does make an instructive contribution to the development of the retinotectal map, then we would expect that this is a genetically regulated process. That this is the case in the zebrafish, there can be little doubt, given the recent report (Lee et al., 2004) that disruption of heparan sulfate synthesis results in a marked disordering of the normally well-segregated dorsal and ventral axons in the ascending optic tract. Heparan sulfate is a known regulator of signal recognition for several receptor-ligand systems, including the ephrins (Lee et al., 2004). The genetic basis of axon order in the optic tract has not been studied in any mammal.

Given wide interspecies variability in observed preordering, and considering that the mouse has emerged as the primary mammalian genetic model for neural development, it would seem useful to have a detailed characterization of the pretarget order in the murine retinofugal system. One report (Hindges et al., 2002), with data confined to the brachium of the superior colliculus (SC), has suggested that such an order may be significant, but the chronologic and spatial development of this order must be established to make this claim. To this end, we undertook a detailed and quantitative axon tracing study in the widely studied C57BL/6 mouse strain. Our results indicate that fiber populations originating from the dorsal and ventral retina become segregated from one another immediately after the chiasm, as reported in some other species, and that this segregation is accomplished by postnatal day 1 (PND1), well before target zones are formed in the SC. On the other hand, we found no evidence of axon sorting according to the position of the parent cell along the nasotemporal axis of the retina. These data suggest that pretarget axon ordering in the optic tract may play an

important role in the development of retinotopic maps in the LGN and SC.

MATERIALS AND METHODS

Animals

We examined mice of the C57BL/6 strain bred in our colony. Two age groups were studied, PND0–1 and PND11–21. Birth time was usually noted within 6 hours, but never at more than 24 hours. Procedures were carried out in accordance with approved protocols from Baylor College of Medicine and NIH guidelines.

Retinal labeling

Pups were anesthetized with an IP injection (0.7 ml/kg) of a combination anesthetic (ketamine 4.28 mg/ml, xylazine 0.82 mg/ml, acepromazine 0.07mg/ml). After the eyelid was surgically opened, the eye was protruded, and a small injection (2.6 nL) of dye (DiI or DiAsp; Molecular Probes, Eugene, OR; 10% in dimethylformamide) was made beneath the sclera. The injection was through a glass pipette attached to a microinjector (Microject II, Drummond Scientific, Broomall, PA). Animals were allowed to recover from the anesthesia, were put back with their mother, and were then sacrificed after 48 hours, or 24 hours for neonatal (PND0) mice. Upon sacrifice, the injected eye was fixed in 10% buffered formalin for later examination to localize the injection site relative to the four major eye muscles (the superior rectus [SR], medial rectus [MR], inferior rectus [IR], and lateral rectus [LR]). Animals with dye injections that spread beyond a focal spot in the retina were eliminated from further analysis. The injection position along the perimeter of the retina was reliably localized to a given one-third of each muscle or intermuscle space, yielding 24 possible injection sites. The intermuscle spaces and the spans of the insertion of the four muscles are not equal; they were measured in three PND14 animals, and the means are indicated schematically in Figure 1.

Distribution of label in whole mount preparations

At the time of sacrifice, the brain was removed and the cerebral cortex was dissected away. Digital images of dye label were acquired under epifluorescent illumination by using a CCD camera and associated software (Epix, Houston, TX).

The SC was imaged by using a 2.5× objective. The position of the target zone of the labeled RGCs in the SC was quantified by first aligning the digital image of the SC on a standard coordinate system by using the midline and the point at which the medial edges of the two colliculi diverge rostrally (Fig. 2A). The center of mass of the fluorescent label (thresholded at 75% of the maximum fluorescence) in the SC was calculated. The position of the center of mass is then considered to be the collicular location of the focal retinal projection, or the target zone. Images were also taken focused on the rostral edge of the SC in order to assess the distribution of axons as they passed into the SC from the brachium.

After the SC and brachium were digitally imaged, the brain was bisected midsagittally, and the half contralateral to the injected eye was oriented with the lateral side up so that the uppermost part of the optic tract could be visualized. This is the region just before the tract reaches the ventral lateral geniculate nucleus and is referred to here as the delta of the optic tract (deltaOT; Fig. 1B). Fluorescent digital images of the deltaOT were obtained by using a 5× objective.

We quantified the axon distribution in the deltaOT and brachium of the SC by using software written in IDL (Research Systems, Boulder, CO) and (MATLAB, Natick, MA). First, a path was defined crossing the tract from the medial to the lateral edge. The fluorescence of the pixels in this path was weakly smoothed with a gaussian filter and recorded as a fluorescence profile (FP), which gives the filtered fluorescence as a function of mediolateral position in the tract. The FP was background-subtracted and normalized by the total area under the FP curve. The position of labeled retinal axons in the tract was quantified by calculating the center of mass of fluorescent label along the defined mediolateral path. A center of mass value of 0 would indicate that all axons lie on the medial edge of the tract, and a value of 1 would indicate that all axons lie on the lateral edge of the tract.

All results are reported as mean ± SEM. Error bars in figures represent the SEM. Means were compared with a Student's t-test and corrected for multiple comparisons when appropriate. Results were considered significant at the $P = 0.05$ level.

Distribution of label in tissue sections

Some mice received both dorsal and ventral injections on the day of birth (PND0), using DiI and DiAsp, in the same eye. On the following day, the animal was anesthetized and sacrificed, and the skin and skull above the SC were removed. At this age, nearly the entire SC is visible because the cortex has not yet made the extensive backward expansion that will eventually obscure much of the SC. Whole mount fluorescence images were taken with filters designed to admit emission from only DiI or DiA. The pair of retinal injections was judged to be successful if the labeled axons from both the dorsal and ventral focal injections were not spread diffusely across the mediolateral extent of the colliculus. In a small number of cases with poor retinal injections the axons from one of the injections were broadly distributed, so the sample was discarded. The entire head of the animal, with the SC exposed, was then fixed in 10% buffered formalin, cryoprotected in 30% sucrose, frozen, and cut at 20 μm, either coronally (to study the optic nerves) or horizontally (to study the optic tract) on the cryostat. The sections were then photographed at 100× or 200× using filters designed to reveal DiI and DiA label.

Horizontal sections were used to study the distribution of dorsally and ventrally labeled RGC axons in the basal optic tract. In this plane of section the axons were cut approximately normal to their direction of travel. All quantified sections were within 200 μm of the chiasm. Axon distribution in the optic nerve was similarly studied in coronal sections, also taken within 200 μm of the chiasm.

The basal optic tract in horizontal section has the shape of a thick comma with a wide blunt rostral end and a tapering, pointed caudal end. In order to quantify the distribution of labeled retinal axons in the section, the basal optic tract was outlined, and an axis was drawn across the widest point, approximately in the mediolateral

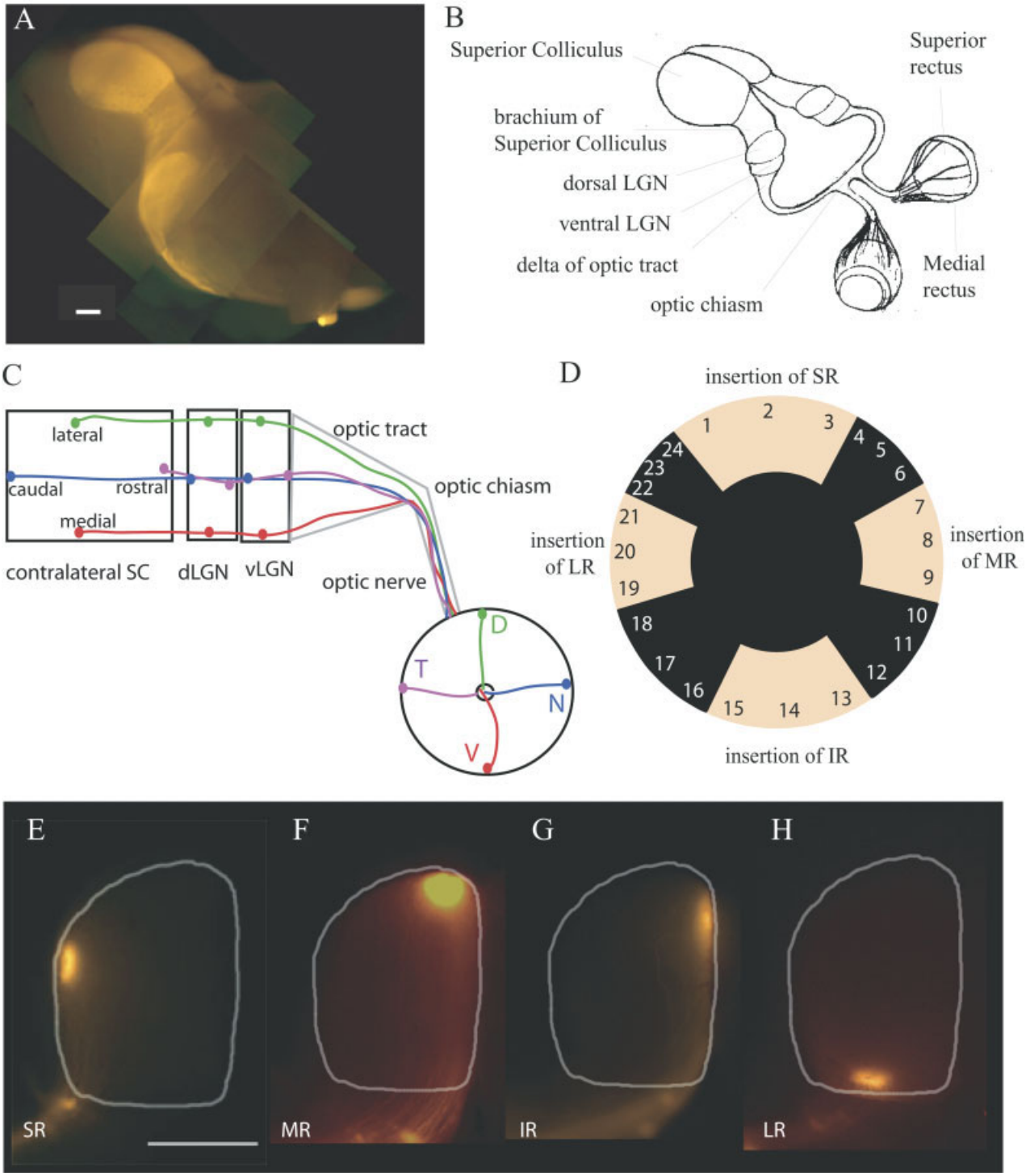

Fig. 1. Ocular muscle anatomy and the retinofugal projection of the mouse. **A:** Vitreal injection of DiI in both eyes reveals the gross form of the retinofugal projection. The overlying cortex and the eyes have been removed from this whole mount fluorescent image. **B:** Schematic of relevant anatomical features of the retinofugal projection in the mouse. Drawing is in approximately the same perspective and scale as A. **C:** Schematic showing the pattern of terminations of dorsal, nasal, ventral, and temporal retinal ganglion cell axons in the dorsal and ventral lateral geniculate nuclei (dLGN and vLGN) and contralateral superior colliculus. Axons enter the targets perpendicular to the mediolateral target axes, corresponding to the dorsoventral axis of the retina. **D:** Schematic of muscle insertion points around the globe of the eye. Oblique muscles are very small in rodent and are not considered. The sizes of both the muscle (sectors 1–3 for superior rectus [SR], 7–9 for medial rectus [MR], 13–15 for inferior rectus [IR], and 19–21 for lateral rectus [LR]) and intermuscle regions (4–6; 10–12; 16–18, and 22–24) are drawn to scale. **E–H:** Injection of dye into the four principal muscles leads to spots of label around the perimeter of the superior colliculus. In E, dye was injected into sector 2 of the superior rectus (SR). In F, dye was injected into sector 8 of the medial rectus (MR). In G, dye was injected into sector 15 of the inferior rectus (IR). In H, dye was injected into sector 20 of the lateral rectus (LR). White lines show outline of the superior colliculus. Medial is to the right, and caudal is up. Scale bars = 1 mm in A,E (applies to E–H).

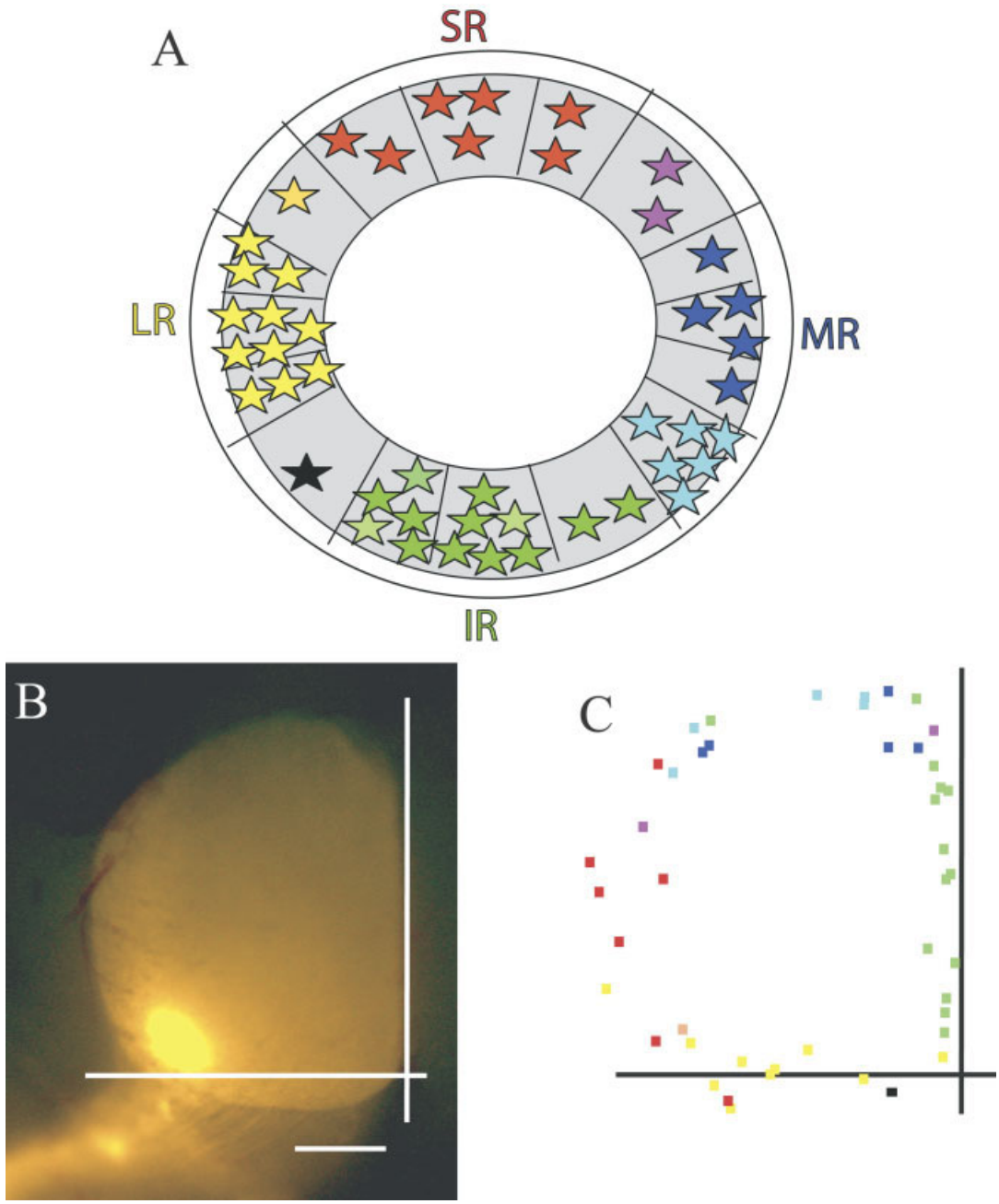

Fig. 2. The collicular projection as a function of retinal location. Using the coordinates defined by the eye muscles in Figure 1D, we performed a series of retinal injections around the periphery of the retina and determined the location of their collicular target zones. **A:** All of the retinal injection sites (n = 45) are shown in eye muscle coordinates. **B:** An example collicular target zone for a temporal retinal injection, with axes (white lines) used to quantify target zone location. **C:** A standard coordinate system, depicted here by black lines, was used to identify the location of the target zone in the superior colliculus. All target zones were measured with respect to the position of the point of divergence of the rostral superior colliculus from the midline (intersection of vertical and horizontal white lines in B). This is analogous to the 'lambda' point in skull coordinate systems. Shown are the positions of all the target zones from the retinal injection sites shown in A, with colors representing retinal location of injection in muscle coordinates as shown in A. Scale bar = 500 μm in B.

direction. The midpoint of this axis was then connected to both the rostral and caudal ends, which divided the tract into roughly equal-sized medial and lateral hemisections. The dorsal and ventral retinal labels were thresholded at 75% of maximum intensity, and the fraction of labeled pixels in each hemisection was calculated. The same quantification procedure was followed for the optic nerve, except we looked for segregation of label in any of eight hemifields (dorsal, ventral, lateral, medial, dorsal-lateral, ventral-medial, dorsal-medial, and ventral-lateral).

RESULTS

The retinofugal projection of the mouse

We examined the retinotopy of retinofugal axons at several anatomical locations, including the optic nerve, optic tract, and brachium of the SC in early neonatal (PND 0) and 2-week-old (PND 14) mice (Fig. 1A,B). The three major topographic targets of the retinofugal projection, i.e., the vLGN, dLGN, and SC, are presented to the optic tract in series, and the tract traverses them along the axis of nasotemporal mapping (Fig. 1C). This anatomical marker, which is true for all vertebrate species examined, implies that the targeting of the nasotemporal coordinate must be reestablished anew in each target. On the other hand, the spatial representation of the dorsoventral axis in each of these targets lies perpendicular to the axons' trajectories in the optic tract. Once dorsoventral order has been established in the first target, it could be sufficient for subsequent targets, as long as it is not lost in the intervening tract.

To analyze quantitatively the routes taken by RGC axons in the retinal projections from different locations within the eye, we established a system of retinal coordinates based on the location of the focal retinal injections relative to the insertion point of the principal eye muscles on the globe of the eye. We targeted the retinal injections to the periphery of the retina, with 34 of 47 injections within 500 μm of the outer edge of the retina, 12 injections within 1,000 μm, and 1 injection between 1,000 and 1,500 μm of the outer edge of the retina (438 ± 34.7 μm from the outer edge on average). We then used the insertions of the principal eye muscles (Fig. 1D) to define a coordinate system for the injections around the circumference of the retina. Focal retinal injections of dye in 2-week-old mice, which have an anatomically mature retinotopic map (Hindges et al., 2002), produced a small spot of label in the SC (Fig. 1E–H). We examined the distribution of labeled retinal ganglion cell axons at different levels of the optic nerve and ascending optic tract (Fig. 1B), including in the optic nerve just before the chiasm, in the optic tract just after the chiasm, in the delta of the optic tract just before the LGN, in the brachium of the SC just before axons enter the SC, and finally in the SC itself.

Retinal locations defined in "eye muscle coordinates" (Fig. 1D) have a predictable and reproducible projection pattern to the SC (Fig. 2). For example, temporal injections (yellow in Fig. 2, in the region of the lateral rectus muscle [LR]), reproducibly produce target zones on the rostral side of the SC. As the injection location moved clockwise from the lateral to the dorsal retina, (red in Fig. 2), the target zone moved to the lateral colliculus. Further clockwise movement of the injection in "eye muscle coordinates" produced commensurate clockwise movement of the target zone in the SC. The muscle coordinate system therefore provides a reliable way of identifying the retinal location of labeled RGCs.

Magnification of the ventrotemporal projection

In the course of characterizing the collicular targets produced by focal injections around the periphery of the retina, we noticed that ventral injections frequently produced target zones that were dramatically elongated along the rostrocaudal axis. Typical focal injections in the retina produced roughly circular target zones in the colliculus. For example (Fig. 3), injections into the dorsal retina (sectors 1–3 in Fig. 1D) produced target zones that were modestly longer on the rostrocaudal axis than on the mediolateral axis of the colliculus (ratio of 1.95 ± 0.18; n = 7; Fig. 3B,D). In contrast, injections into the ventrotemporal retina (sectors 15–18) produced target zones that were very elongated along the rostrocaudal axis of the colliculus (ratio of 8.23 ± 1.99; n = 6; $P < 0.01$; Fig. 3A,D). Injections into the neighboring ventronasal retina (sectors 13–14) produced target zones (ratio of 2.84 ± 0.48; n = 8; Fig. 3C,D) that were not significantly elongated relative to the dorsal retina (sectors 1–3) and were much less elongated ($P < 0.01$) than in the ventrotemporal retina (sectors 15–18). Thus, a very limited region of the ventrotemporal retina produced target zones that were much more elongated than in other regions of the retina, even nearby injections into the ventronasal retina. It is interesting to observe that the region of dramatically elongated projections to the colliculus corresponds to the field of binocular vision that receives input from both ipsilateral and contralateral retinas.

Retinotopic order of dorsoventral axons in the ascending optic tract

In mice with mature retinotopic maps (PND 11–21), we first examined the distribution of axons from different retinal locations at the brachium of the SC, which is just before axons enter their final target. Order at the brachium of the SC has been previously noted in the rat (Simon and O'Leary, 1992) and in the mouse (Hindges et al., 2002). Using eye muscle coordinates to quantify this order (Fig. 4), we found that the mediolateral order of retinal axons in the brachium of the SC reflected their dorsoventral (DV) origin in the retina. At PND11–21, axons from the dorsal retina were highly lateralized in the brachium (Fig. 4A,E), whereas axons from the ventral retinal ran in the most medial aspect of the brachium (Fig. 4B,E). Axons originating from nasal or temporal retinal origins tended to have a similar distribution within the center of the brachium (Fig. 4C–E). A summary of these data is shown in Figure 4F, where the center of mass (CofM) of axon label in the brachium (see Materials and Methods) is shown as a function of retinal origin in eye muscle coordinates. RGC axons originating near the superior rectus (dorsal axons) were lateralized (CofM = 70% ± 2% of the mediolateral distance; n = 7) in the brachium relative to axons originating near the inferior rectus (ventral axons; CofM = 26% ± 1%; n = 10; $P < 0.001$). In contrast, axons originating near the medial or lateral rectus ran centrally in the brachium with a statistically indistinguishable center of mass location ($P = 0.34$).

We wondered whether ordering of axons at the brachium of the colliculus could possibly be an indirect effect of interactions between axons and their nearby target in the SC (or even interactions at the LGN, which the axons already passed through). We therefore analyzed the topography of axons at the delta of the optic tract (deltaOT), which is found before the axons reach the LGN or any other synaptic target (Fig. 5). At PND 11–21, axons from the dorsal and ventral retina were well sorted in the deltaOT (Fig. 5A,C,E), with dorsal axons running on the lateral edge of the contralateral optic tract (Fig. 4A). Ventral axons that originated from the middle third of the inferior rectus ran on the medial edge of the deltaOT (Fig. 5C). In contrast, axons from the nasal and temporal retina

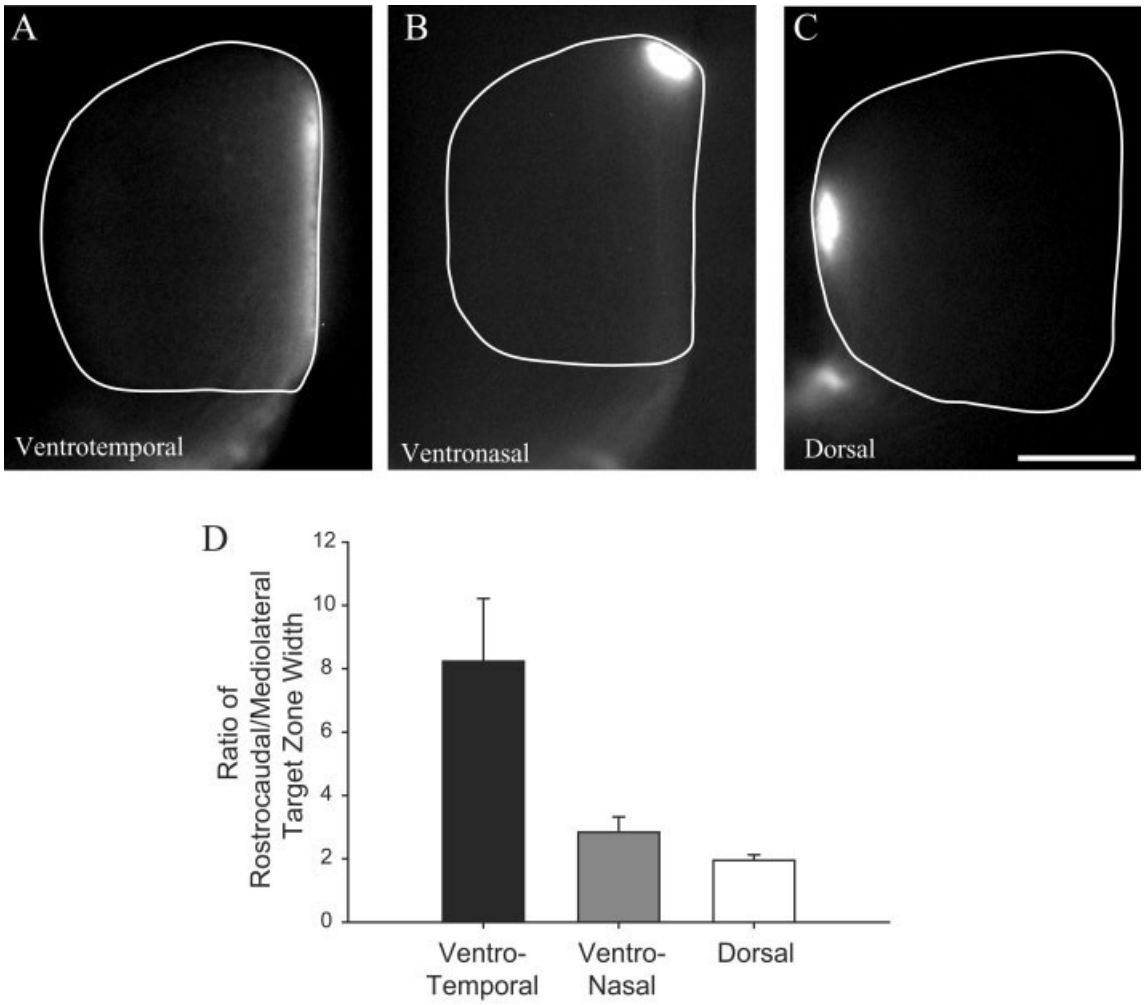

Fig. 3. Elongation of ventrotemporal retinal targets in the superior colliculus. **A:** The collicular target zone from axons originating from ventrotemporal retinal (sectors 15–18 in Fig. 1D) shows a characteristic elongation along the rostrocaudal axis. **B:** Target zones originating from neighboring ventronasal retina (sectors 13–14 in Fig. 1D) are much less elongated. **C:** Target zones from axons originating from dorsal retina (sectors 1–3) are also much less elongated than those from ventrotemporal retina. **D:** Quantification of the target zone elongation along the rostrocaudal relative to mediolateral dimension due to injections in ventrotemporal (n = 6; black bar), ventronasal (n = 8; gray bar), and dorsal (n = 7; white bar) retina. Medial is to the right, and caudal is up. Scale bar = 500 μm in C (applies to A–C).

(from the middle third of the medial rectus and lateral rectus, respectively) overlapped in the middle of the deltaOT (Fig. 5B,D,F). The distribution of axons across the deltaOT for axons originating from the dorsal and ventral retina is shown in Figure 5E, where it is apparent that the two groups are well segregated in the optic tract. In contrast, axons originating from the nasal or temporal retina overlapped and were more broadly distributed across the center of the optic tract. A summary quantification of the center of mass of these distributions (Fig. 5G) clearly shows that dorsal and ventral axons run on the lateral (CofM = 76% ± 2% of the mediolateral distance; n = 3) and medial (CofM = 30% ± 2%; n = 5) edge of the optic tract, respectively. Dorsal (SR) axons were significantly more lateralized than ventral (IR) axons ($P < 0.001$). In contrast, nasal (MR) and temporal (LR) axons had a similar distribution (CofM = 56% ± 2% for n = 2 nasal injections; CofM = 63% ± 2%; for n = 4 temporal injections; $P = 0.36$) in the midoptic tract that was significantly different than the distribution of dorsal or ventral axons ($P < 0.05$).

Sorting of RGC axons occurs prior to target formation

We have demonstrated that at a time when the retinotopic map is anatomically mature in the SC (PND11–21), the dorsoventral origin of retinal axons is reflected in their position in the optic tract at both the brachium of the superior colliculus and the deltaOT. In contrast, axons originating from the nasal and temporal retina show no positional bias. In order for this pretarget sorting to be instructional, it must precede the formation of target zones in the colliculus. We therefore investigated whether pretarget order exists at PND1, a time when axons have invaded the colliculus but have not yet arborized or formed target zones (Fig. 6A; (Hindges et al., 2002). Al-

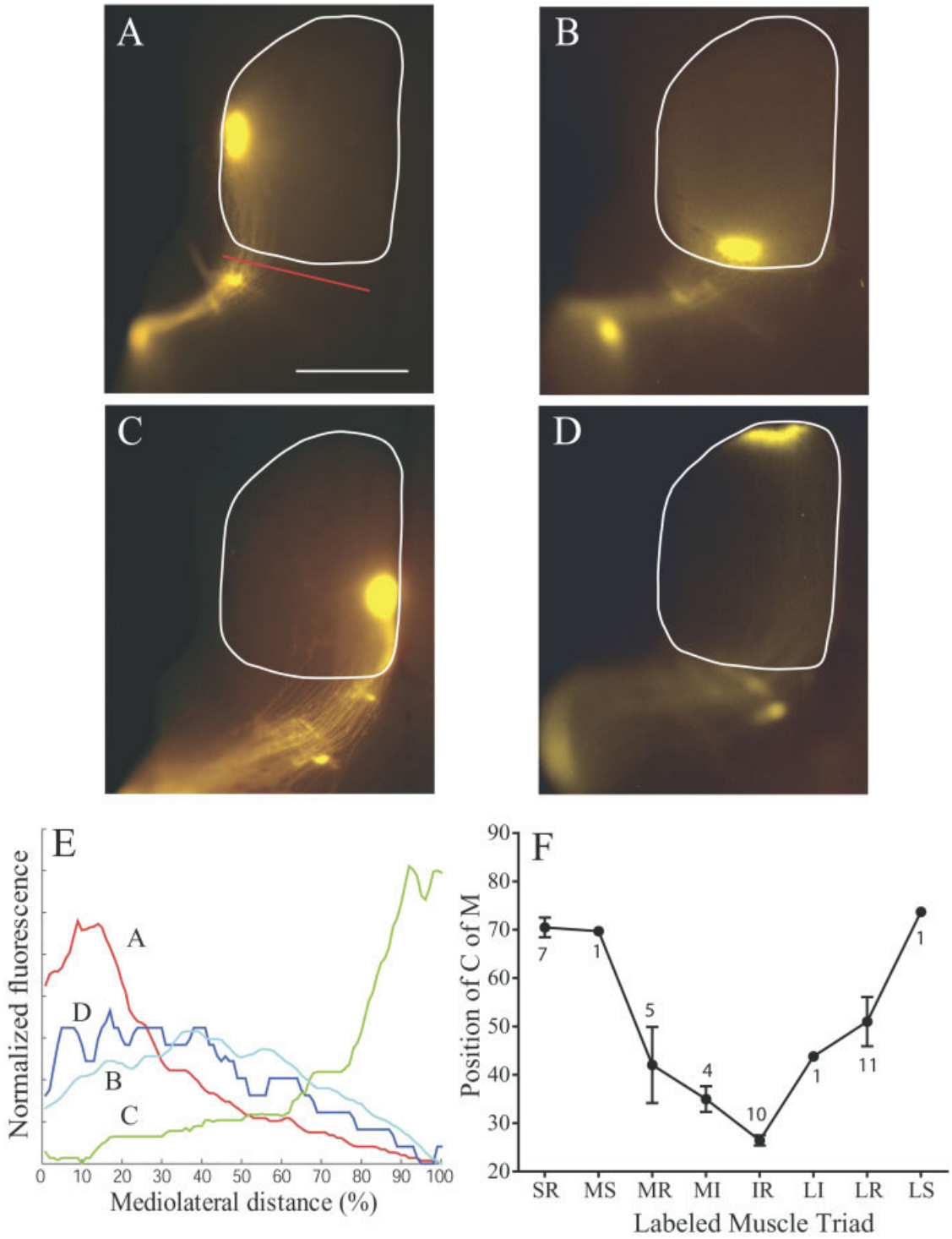

Fig. 4. The mediolateral order of axons in the brachium of the superior colliculus reflects their dorsoventral origin in the retina. **A:** Axons originating from dorsal retina (SR) are strongly biased to enter the SC (outlined) from the lateral side. The diagonal line (red) indicates the path across the brachium in which axonal labeling was measured. **B:** Axons originating from temporal retina (LR) are not biased to either the lateral or medial colliculus on entry. **C:** Axons from ventral retina (IR) are strongly biased to enter the colliculus on the medial edge. **D:** Axons originating from the nasal retina (MR) show no medial-lateral bias upon entry into the colliculus. **E:** Normalized distribution of fluorescent label in the brachium for the four animals represented in A–D. **F:** Average position of the center of mass of the distribution of fluorescent label in the brachium as a function of retinal location of the injection. Position of the center of mass of the fluorescent label is shown as a function of total medial-lateral width of the brachium, such that 0% means the average center of mass is on the medial edge, and 100% means the average center of mass of the distribution of fluorescent label is on the lateral edge. The location of the retinal injection (abscissa) is defined in muscle coordinates. The four principal ocular muscles (SR, MR, IR, and LR) are indicated, along with the intervening intermuscle regions (MS, MI, LI, and LS). The number of animals (injections) appears next to the corresponding point in the plot. Medial is to the right, and caudal is up. Scale bar = 1 mm in A (applies to A–D).

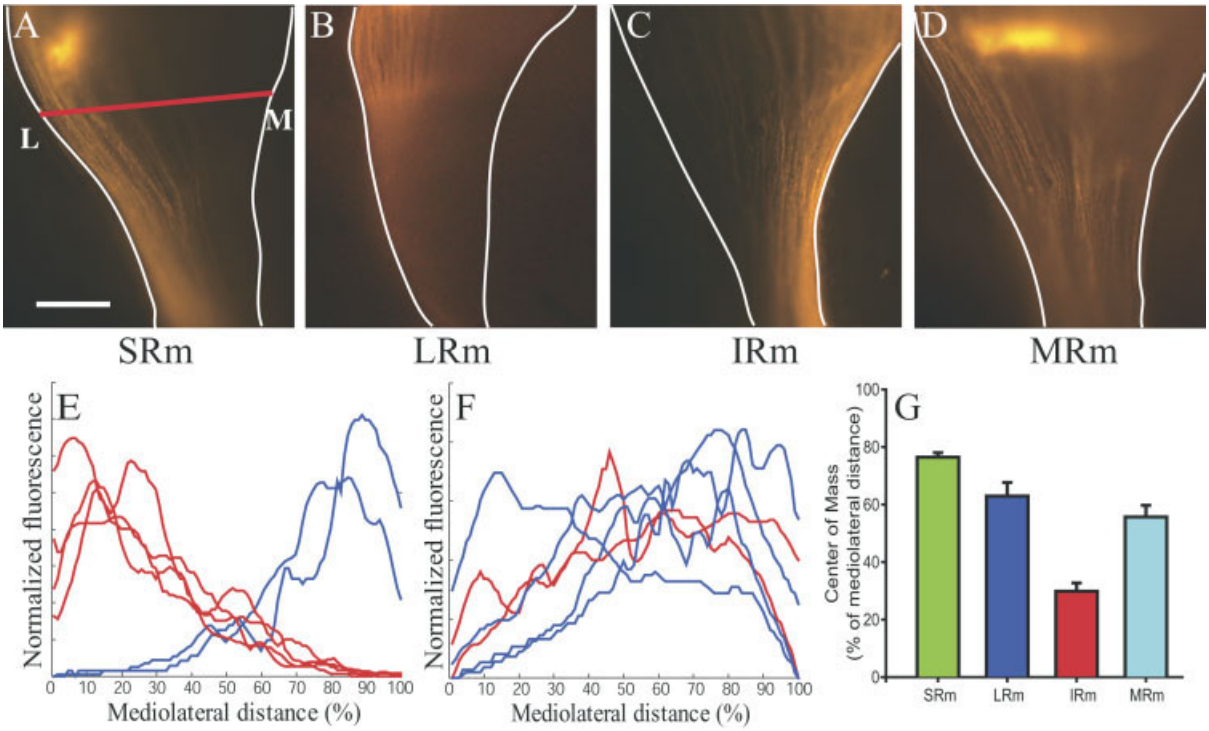

Fig. 5. Position of RGC axons in the delta of the optic tract as a function of retinal origin. **A–D:** Axons originating from dorsal (A) or ventral (C) retina travel in the lateral or medial optic tract, respectively, whereas axons from nasal (D) or temporal (B) retina show a broader, more central distribution.. The target zone in the ventral LGN is visible in A and D. **E:** Distribution of label in the optic tract for ventral (red, n = 4) and dorsal (blue, n = 3) injections. Dorsal (blue) injections are lateralized, and ventral (red) injections are in medial optic tract. **F:** Distribution of label in optic tract for nasal (red, n = 2) and temporal (blue, n = 4) injections. No difference in the distribution of label in the optic tract for the nasal (red) and temporal (blue) injections is apparent. **G:** Quantification of axon order in optic tract. Position of the center of mass of labeled axons for the four "polar" retinal injection locations. Injections in the dorsal retina (SR sector 2; green bar) result in label that is much more ($P < /I < 0.001$) lateralized than injections into ventral retina (IR sector 14, red bar). No difference in label distribution is seen for nasal (MR sector 8, light blue) and temporal (LR sector 20, dark blue) injections, but the center-of-mass of label for the nasal and temporal injections is different from that in either the dorsal or ventral injections ($P < 0.01$). Scale bar = 200 μm in A (applies to A–D).

though target zones have not formed at PND1, there was still a clear tendency for axons originating from the dorsal retina to enter the SC on its lateral edge and run parallel to the midline (Fig. 6A,B). Similarly, axons from the ventral retina entered the colliculus on its medial edge and ran up the midline on the opposite side of the colliculus from dorsal axons (Fig. 6A,C). Summary quantification of this separation in singly injected animals confirmed this effect: RGC axons originating from the dorsal retina were significantly more lateralized than ventral originating axons in the SC (mean CofM, ventral 38 ± 0.9% of the SC mediolateral width; n = 8; dorsal, 63% ± 1.94% of the SC mediolateral width; n = 8; $P < 0.001$). Axons from the dorsal or ventral retina at PND1 were more confined along the ML axis of the colliculus than along the RC axis. Examination of dorsal (Fig. 5D) and ventral (Fig. 5E) injections revealed that the mediolateral extent of the axon label for a dorsal or ventral injection was much less (33.0 ± 4.8% of the SC width) than the rostrocaudal extent (55.8 ± 4.3% of the SC length; $P < 0.001$ for n = 12 injections). Thus, axon targeting in the SC is already quite accurate at PND1 across the mediolateral axis but is much coarser across the rostrocaudal axis.

Segregation of dorsal and ventral RGC axons at PND1 in the ascending optic tract was also apparent when we examined the deltaOT (Fig. 7). Dorsal axons (Fig. 7A,C) were strongly biased toward the lateral side of the optic tract (CofM of label at 70 ± 1.4% of the medial-lateral extent; n = 8), whereas ventral axons (Fig. 7B,D) were biased toward the medial edge of the tract (CofM of label at 31% ± 1.0% of the mediolateral extent; n = 8; $P < 0.001$). Thus, the distribution of axons in the optic tract before they have reached a central target reflects their dorsoventral origin in the retina.

We examined whether the segregation of axons observed in the deltaOT, near the LGN, was already established at PND1 at a point where the axons exit the optic chiasm at the very base of the optic tract (Fig. 8). This was more difficult to assay than at more central locations in the optic tract, as the nerve is quite compact near the chiasm and twists as it ascends the side of the brain. We used horizontal sections, which roughly transect the nerve near the base of the brain. We also used paired injections of different fluorescent tracers (DiI and DiA) in the dorsal and ventral retina, which was more reliable because it allowed us to compare the distribution of both dorsal and ventral axons in the same optic tract. We found in these sections that axons originating from the ventral retina (Fig. 8A) tended to lie in the lateral aspect of the optic tract, whereas axons from the dorsal retina (Fig. 8B) were

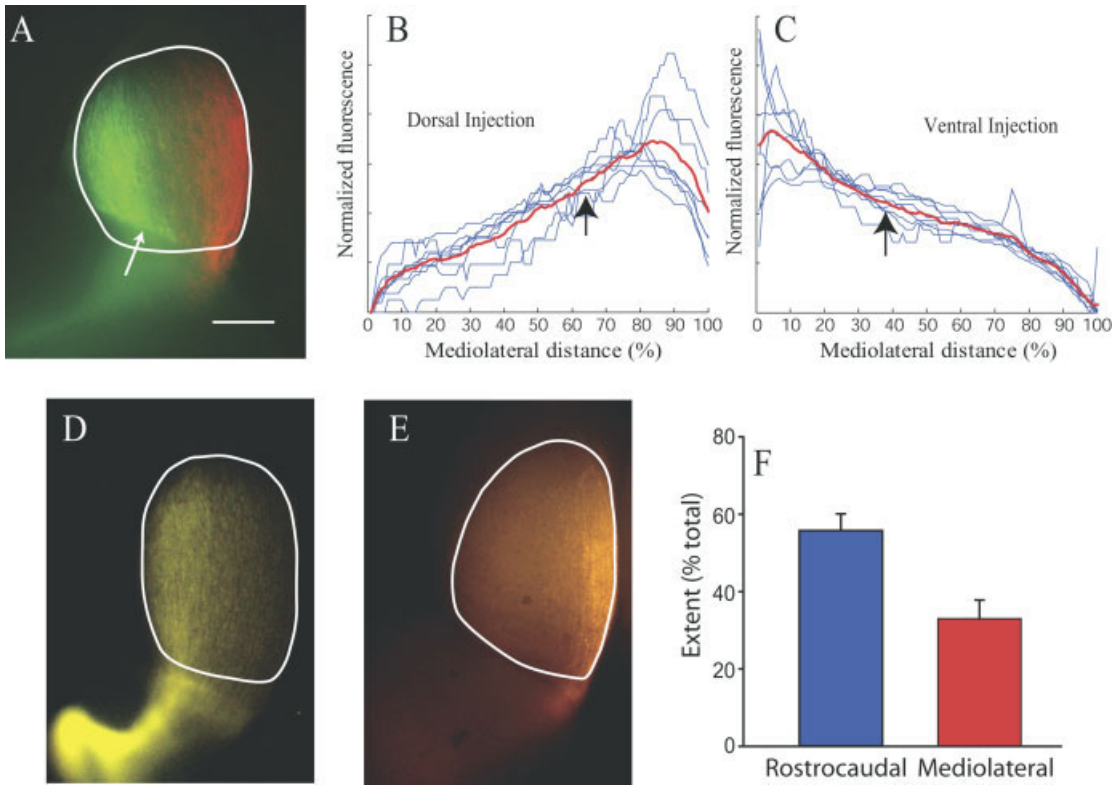

Fig. 6. Segregation of DV axons in the superior colliculus at PND1. The day after birth (PND1), the majority of RGC axons have invaded the SC, but the future target zone of a focally labeled population of RGC axons is not yet discernible. Nonetheless, the mediolateral extent of the presumptive target zone is already defined by the mediolateral extent of the invading axons. **A:** Example of a superior colliculus labeled by a doubly injected retina (dorsal green, ventral red) at PND1. Overlying cortex partly obscures the rostral colliculus at the white arrow. **B,C:** Axons labeled after focal injection into dorsal (B) or ventral (C) retina travel in the lateral or medial SC, respectively. Black arrows indicate the average center of mass of these distributions. Axons from the dorsal retina are more lateral ($P < 0.001$) than axons from the ventral retina. **D:** Example of PND1 SC after a dorsal retinal injection illustrates that axons are quite confined in the mediaolateral plane but stretch nearly the entire rostrocaudal extent of the SC. **E:** Example of a PND1 SC after a ventral injection, showing again that axons are confined mediolaterally but extend nearly the entire rostrocaudal length of the SC. **F:** Quantification of the difference between the mediolateral and rostrocaudal extent of axon label after confined dorsal or ventral injections into retina. The mediolataral spread (width at ¾ height) of axon label in the SC is much less ($P < 0.001$) than the rostrocaudal spread. Medial is to the right, and caudal is up in all panels. Scale bar = 500 μm in A (applies to A,D,E).

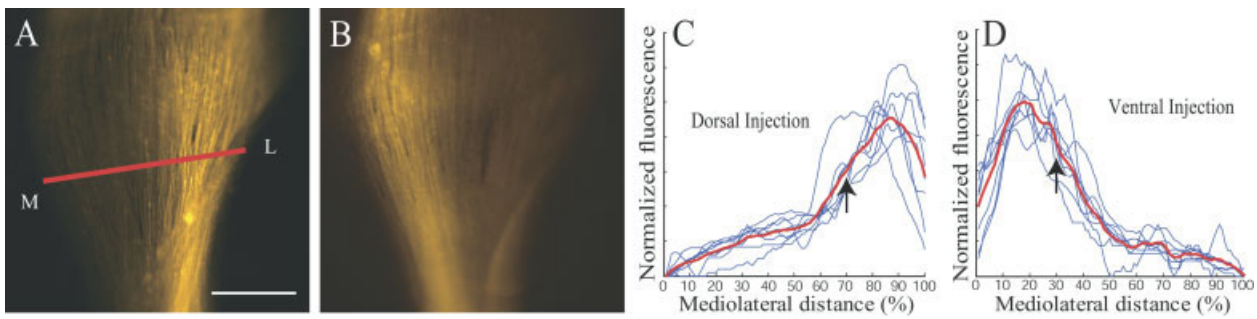

Fig. 7. Segregation of DV axons in the optic tract (deltaOT) at PND1. Axons labeled after focal injection into dorsal or ventral retina travel in the lateral or medial optic tract, respectively. **A:** Example of axon label in the delta of the optic tract after a dorsal retinal injection. Red line indicates where quantification of fluorescent label across the optic tract is performed. Medial is left, and lateral is right. **B:** Example of axon label in the delta of the optic tract after a ventral injection. Again, medial is left, and lateral is right. Note that the label is shifted toward the medial side of the tract. **C:** Profile of the fluorescent label in the delta of the optic tract for (n = 8) dorsal injections. **D:** Profile of the fluorescent label in the delta of the optic tract for (n = 8) ventral injections. Black arrows in C and D mark the mean of the center of mass of the fluorescent label, which is much different for the dorsal (C) and ventral (D) injections ($P < 0.001$). Scale bar = 250 μm in A (applies to A,B).

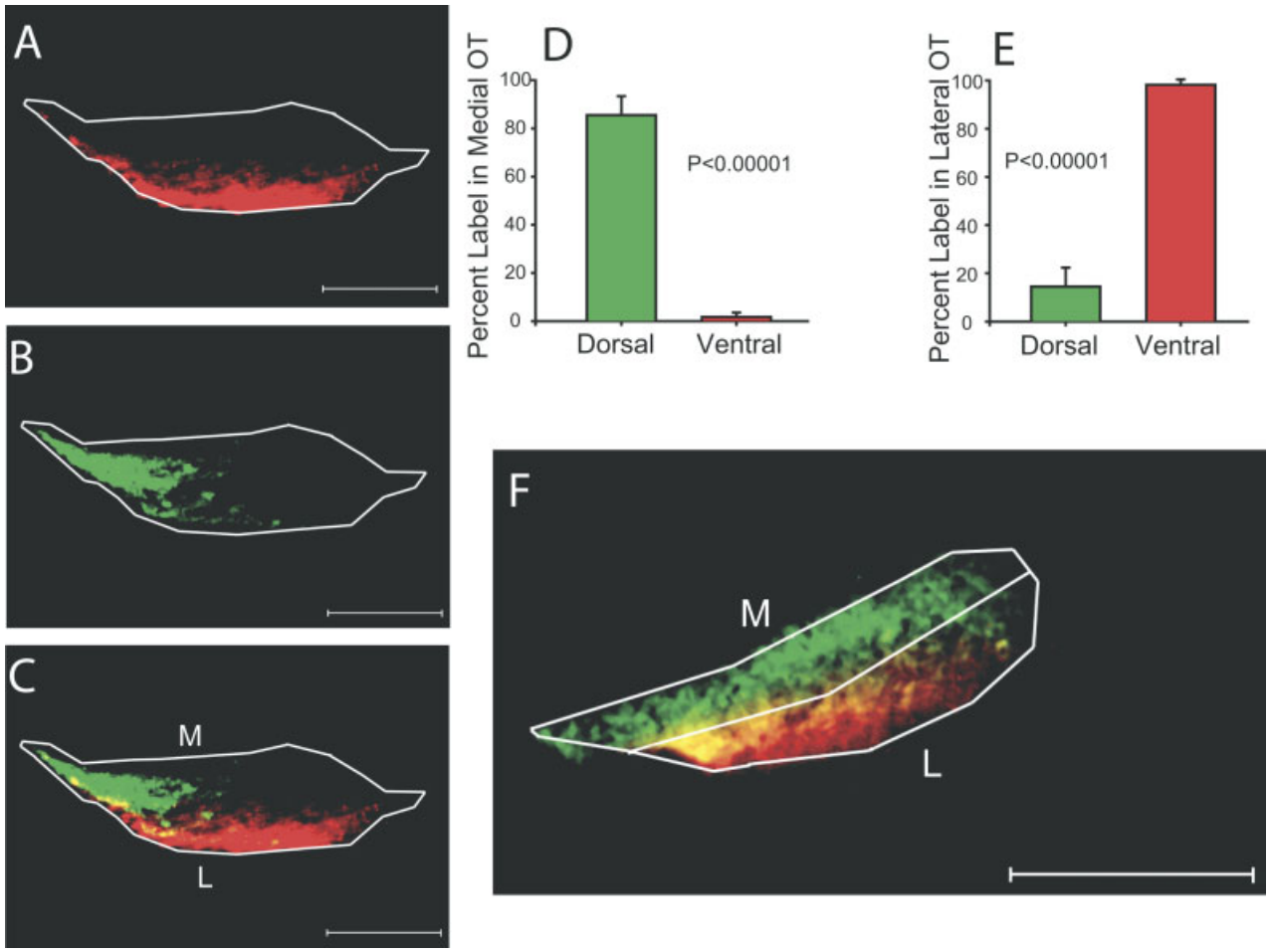

Fig. 8. Position of dorsal and ventral axons in the basal optic tract at PND1. Animals received paired ventral (**A**, red) and dorsal (**B**, green) injections in one eye on the day of birth. Horizontal sections of the optic tract within 200 μm of the optic chiasm reveal a spatial segregation of the two labels (A, B, overlay in **C**). Another example is shown in **F**, to illustrate the division of the tract into medial and lateral sectors for quantitative comparison. Rostral is to the right in A–C and F. Quantification of the distribution of label for the top quartile of fluorescence shows a differential distribution of dorsal and ventral label in the medial (**D**) and lateral (**E**) halves of the tract, with dorsal axons running preferentially in the medial optic tract and ventral axons in the lateral optic tract. Scale bar = 125 μm in A–C,F.

in the medial tract. A second example of this pattern is shown in Figure 8F. On average (n = 5 in all cases), 86 ± 7.8% of the dorsal retinal ganglion cell label was in the medial optic tract (see Materials and Methods), whereas only 1.8 ± 1.8% of the ventral retinal ganglion cell label was in the medial optic tract (Fig. 8D; $P < 0.00001$). In contrast, only 14.5 ± 7.8% of the dorsal retinal ganglion cell label was in the lateral optic tract, whereas 98 ± 1.8% of the ventral retinal ganglion cell label was in the lateral optic tract. Ventral retinal ganglion cell label was not restricted to either the rostral or caudal tract, but there was a tendency for dorsal retinal ganglion cell label to localize preferentially to the caudal tract (89 ± 6%; $P < 0.0001$). Thus, just past the chiasm, dorsal and ventral axons tended to occupy distinct zones within the ascending optic tract.

No order in the optic nerve

In contrast to the optic tract, axon order was not visible in the optic nerve at a point just proximal to the optic chiasm (Fig. 9). Using the same double labeling methodology and quantification as was used in the optic tract, we examined the distribution of axons from the dorsal and ventral retina within the last 200 μm of the optic nerve before the optic chiasm was reached at PND1. Axons in the optic nerve near the chiasm were quite broadly distributed, without any consistent order or segregation within the nerve, and with a highly variable distribution from case to case. In the optic tract (Fig. 8), segregation between the medial and lateral tracts was obvious by visual inspection. In contrast, there was no obvious restriction of either dorsal or ventral label to any particular region of the optic nerve. We checked for segregation of dorsal (Fig. 9A,D) and ventral (Fig. 9B,9F) axons in the dorsal nerve (19 ± 7% dorsal retinal label; 24 ± 6% ventral retinal label), ventral nerve (31 ± 6% dorsal retinal label; 26 ± 7% ventral retinal label), medial nerve (19 ± 4% dorsal retinal label; 22 ± 7% ventral retinal label), and lateral nerve (31 ± 6% dorsal retinal label; 28 ± 6% ventral retinal label) hemisections (n = 5), and no segre-

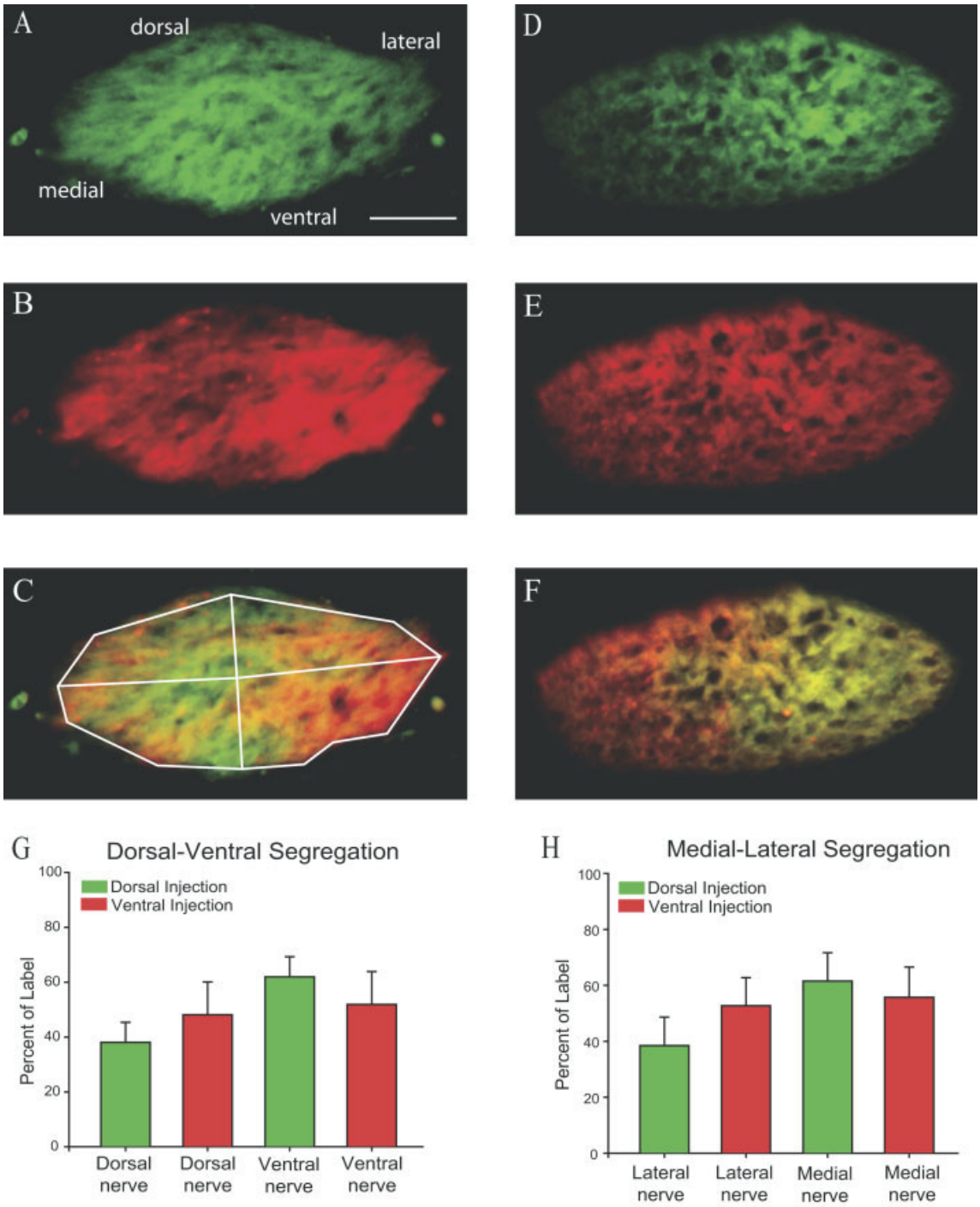

Fig. 9. Position of dorsal and ventral axons in the optic nerve near the chiasm at PND1. The same analysis of the distribution of label done for the optic tract (Fig. 8) was performed on the optic nerve within 200 μm of the optic chiasm, with no consistent preference for label of dorsal (shown in green) or ventral (shown in red) axons in any sector of the nerve. **A–C:** Pattern of axons in the optic tract of a PND1 mouse whose eye was injected dorsally (A, green) and ventrally (B, red) on the day of birth. C is the overlay. **D–F:** A similar series of data for a second animal reveals a very different distribution of label, with no consistent pattern between animals. Whether the optic nerve is divided into dorsoventral (G) or mediolateral (H) halves, no statistically significant difference in the distribution of the labels can be distinguished. The 0rientation of section (dorsal up, ventral down, medial left, and lateral right) shown in A applies to A–F. Scale bar = 50 μm in A (applies to A–F).

gation was found (Fig. 9G,H). Because division of the optic nerve into dorsal and ventral or medial and lateral hemisections is arbitrary, we also examined segregation in oblique hemisections (dorsal-lateral, dorsal-medial, ventral-lateral, and ventral-medial). Again, no restriction of label was found. Axon order with respect to dorsal or

ventral origin was therefore absent in the optic nerve and appeared to emerge at or just after the optic chiasm.

DISCUSSION

In this report, we have demonstrated that axonal order in the optic tract, representing the dorsoventral origin of axons in the mouse retina, emerges just after the chiasm. To examine this order quantitatively, we developed a "muscle map" of the eye, which allowed us to determine definitively the retinal origin of labeled axons in the optic nerve and tract. At the time of a "mature" tectal map (PND 14), we showed that there is clear axon order or segregation in the brachium and the deltaOT for dorsal and ventral axons but not nasal and temporal axons. We also showed that before map maturation (PND 1), when RGC axons have only just arrived at the SC and have not begun to branch, axons are already sorted in the optic tract with respect to origin along the dorsoventral axis of the retina but not the nasotemporal axis. We showed that this order is not apparent in the optic nerve before axons enter the chiasm but that axons are segregated just after they emerge from the chiasm, demonstrating that sorting occurs at or near the chiasm. Finally, we demonstrated that the chronological development of this axonal ordering is such that it may play an important role in the development of synaptic topography in the retinofugal targets.

Axon order emerges at the optic chiasm

When retinal ganglion cell axons exit the retina and enter the optic nerve head, they are initially sorted with respect to their retinal origin, with dorsal RGC axons dorsal in the nerve head and ventral axons ventral in the nerve head (reviewed in Jeffery, 2001). Interestingly, this order is soon lost, so that by the time axons near the optic chiasm, they are diffusely spread through the nerve and show no consistent order. Our data show that order emerges again after the axons exit the chiasm. It is curious that axon order is first lost and then regained. It may be that interactions between RGC axons and factors at the chiasm are responsible both for establishing retinotopic order and for executing the crossing decision. Alternatively, there may be distinct signals mediating routing and sorting. For example, axons may change the expression or localization of receptors and/or ligands when they encounter the midline (Thomas, 1998), causing the reemergence of retinotopic order after the midline. Evidence suggests that there may be two classes of ventrotemporal RGCs whose distinct transcription factor expression profiles determine whether they cross the midline (Herrera et al., 2003; Pak et al., 2004). By analogy with the crossing at the midline in the insect that is mediated by a Comm-Robo interaction (Couch and Condron, 2002), one class of these axons is sorted by a midline signal upon approaching the chiasm, whereas the second class does not experience this sorting signal because it is suppressed. Once midline crossing occurs, the suppression of axon ordering signals in the optic tract is released, and order with respect to retinal origin reemerges. Implicit in this process is the interaction of "crossing" signals with "ordering" signals in the RGC axons. A specific example of the mechanism by which this may occur is the regulated expression and trafficking of EphB receptors by RGC axons interacting with an ephrinB sorting signal at the chiasm. In this model, repulsion at the midline by an EphB/ephrinB interaction produces ipsilaterally projecting axons that are pushed to the lateral optic tract. Contralateral projecting axons, in contrast, would not interact with the ephrinB signal at the midline until after they have crossed, when they would again be pushed to the lateral optic tract. Such a crossing-dependent expression of EphB1 has been reported in the development of mouse spinal cord (Imondi et al., 2000; Imondi and Kaprielian, 2001).

Progressive emergence of DV order in the optic tract

Due to the anatomy of the retinofugal projection at the chiasm and ascending optic tract, we were forced to use separate measures of DV order in the optic tract just after the chiasm and the deltaOT, near the entry into the LGN. Nonetheless, retinotopic order is more apparent at the deltaOT than at the chiasm. This feature suggests that, although the initial segregation of dorsal and ventral axons emerges at the chiasm, further mechanisms are responsible for refining this order as the axons ascend the side of the brain. The retinotopic refinement may be due to interactions between dorsal and ventral axons themselves (Birgbauer et al., 2001) or to external guidance factors that influence axon order along the ascending tract. The former possibility is attractive given the complementary expression gradient of ephrinB ligand and EphB receptor along the DV axis of the retina (Peters, 2002), and this form of progressive fiber sorting by axon-axon interactions through inhibitory Eph-ephrin signaling has been described in the invertebrate (Kaneko and Nighorn, 2003). A complementary gradient of ephrinA ligand and EphA receptor also exists along the nasotemporal NT axis of the retina (Hornberger et al., 1999), but it is not thought to be causative in mapping of nasotemporal axis retinal ganglion cells onto the tectum (Yates et al., 2001). If EphB receptors are not trafficked to ventral RGC axon growth cones until after they have crossed the midline (IMondi et al., 2000; Imondi and Kaprielian, 2001), axon-axon interactions among dorsal and ventral retinal ganglion cell axons may also explain why retinotopic order does not emerge until after the optic chiasm.

Mechanisms

Recent experiments have identified some of the early morphogenic signals that are responsible for the establishment of DV polarity in the retina (Koshiba-Takeuchi et al., 2000). In particular, an early high-dorsal to low-ventral gradient of BMP4 in the eye is believed to be the primary dorsalizing cue in the retina. Experimental evidence suggests that a complex cascade of transcription factors and regulators culminates in the differential expression of specific proteins along the DV axis of the retina (Peters, 2002). These include the EphB/ephrinB receptor-ligand system, so it is tempting to speculate that these are also responsible for pretarget order in the optic tract. However, a completely separate molecular system may be responsible for pretarget order, with the role of EphB/ephrinB signaling in DV axis retinotopy limited to the target itself. Although the molecular mechanisms responsible for pretarget order are as yet unknown, recently it was demonstrated in zebrafish that disruption of heparan sulfate expression disturbs pretarget order in the optic tract (Lee et al., 2004). In vitro studies have shown that many receptor-ligand signaling pathways that directly influence axon guidance are modulated by heparan sulfate

expression, including Eph/ephrin, Slit/Robo, Netrin/DCC, and others (Lee and Chien, 2004). Furthermore, the sorting of ipsilateral and contralaterally projecting axons at the chiasm is strongly influenced by EphB/ephrinB signaling (Nakagawa et al., 2000; Williams et al., 2003). It is thus possible that pretarget sorting and chiasm sorting share common signaling pathways.

Pretarget sorting common to all vertebrate species

We have presented evidence for substantial pretarget order in the optic tract for axons along the DV axis of the retina in the mouse. Similar pretarget order has been previously observed in many species, including the rat, ferret, cat, primate, and marsupials, as well as all the submammalian orders for which it has been examined (Bunt and Horder, 1983). In general, pretarget order is stronger in submammalian orders and has been described as weakest in rodents (Chelvanayagam et al., 1998), although we have shown here that it is quite robust. In the human, clinical literature suggests little fiber order in the optic nerve but an increasing degree of order in the ascending optic tract (Miller and Newman, 1998). In mammals in general (rat, ferret, and cat), order of axons in the optic tract is similar to that reported here, with a more obvious order of axons along the dorsoventral axis of the retina and not along the nasotemporal axis. Generally though, the results appear to be dependent on the specific method used, with anecdotal evidence of order the norm. We have adopted a quantitative methodology that is amenable to comparison both across species and between different genotypes within the same species.

Model for establishment of retinotopy

It is striking that pretarget order appears to be limited to the DV axis of the retina. It is also interesting to note that evidence for Sperry-like interactions via EphA/ephrinA receptor-ligand signaling in the SC for axons along the nasotemporal axis of the retina is very strong (Wilkinson, 2001), but evidence for similar interactions (perhaps via EphB/ephrinB signaling) for retinal ganglion cells along the DV axis of the retina is relatively weak (Hindges et al., 2002). One possibility is that pretarget ordering of DV axis axons is only the first in a multistep process that establishes precise retinotopy in the SC. In this model, fibers enter the colliculus within a "competence zone" relative to the final target zone. Fibers within this zone are then competent to respond to classic within-target chemoaffinity cues, enabling them to undergo selective branching to form the topographically correct target zone. The implication is that neither local, target-based chemoaffinity nor pretarget sorting is sufficient for the proper formation of the retinotectal map. Axon-target interactions may be unable to exert their influence if the initial targeting of axons in the first step is grossly incorrect, and axons outside of this initial first step "competence zone" would be eliminated (Simon and O'Leary, 1992). The final step in this process is activity-dependent refinement of axons via spontaneous retinal waves (Feller, 2002; Grubb et al., 2003; Chandrasekaran et al., 2005). This multistep process may be limited to only the final two steps for nasotemporal axis mapping, as pretarget order appears to be absent for these axons. One implication of this is that if activity-based refinement (correction) were eliminated, then deficits in nasotemporal refinement should be much more severe than DV refinement, which is what has been reported in the literature (Grubb et al., 2003; Chandrasekaran et al., 2005).

Does pretarget order cause retinotopy at the target?

The existence of RGC axon order in the optic tract strongly suggests that molecular factors influence the development of retinotopy well before axons reach their synaptic target. It is difficult to prove that axon order in the optic tract causes retinotopic mapping in the target (SC or LGN), because it is difficult to disrupt pretarget order specifically and not also affect mapping mechanisms at the target. On the other hand, the converse is also true: it is difficult to prove that pretarget order is not necessary for map formation, and experiments specifically disrupting molecular interactions at the target without disrupting pretarget order have also not been done. Thus, we cannot say definitively whether pretarget order is essential for the establishment of target retinotopy, but at a minimum, its existence implies that Sperry-like interactions at the target have less "work" to do.

ACKNOWLEDGMENTS

We gratefully acknowledge John Maunsell, David Sparks, and the members of our lab for helpful discussions and comments on the article.

LITERATURE CITED

Attardi DG, Sperry RW. 1963. Preferential selection of central pathways by regenerating optic fibers. Exp Neurol 7:46–t; 64.

Birgbauer E, Oster SF, Severin CG, Sretavan DW. 2001. Retinal axon growth cones respond to EphB extracellular domains as inhibitory axon guidance cues. Development 128:3041–3048.

Bunt SM, Horder TJ. 1983. Evidence for an orderly arrangement of optic axons within the optic nerves of the major nonmammalian vertebrate classes. J Comp Neurol 213:94–114.

Chan SO, Guillery RW. 1994. Changes in fiber order in the optic nerve and tract of rat embryos. J Comp Neurol 344:20–32.

Chandrasekaran, AR, Plas DT, Gonzalez E, Crair MC. 2005. Evidence for an instructive role of retinal activity in retinotopic map refinement in the superior colliculus of the mouse. J Neurosci. 25:6929–6938.

Chelvanayagam DK, Dunlop SA, Beazley LD. 1998. Axon order in the visual pathway of the quokka wallaby. J Comp Neurol 390:333–341.

Couch J, Condron B. 2002. Axon guidance: Comm hither, Robo. Curr Biol 12:R741–742.

Dunlop SA, Tee LB, Beazley LD. 2000. Topographic order of retinofugal axons in a marsupial: implications for map formation in visual nuclei. J Comp Neurol 428:33–44.

Feller MB. 2002. The role of nAChR-mediated spontaneous retinal activity in visual system development. J Neurobiol 53:556–567.

Grubb MS, Rossi FM, Changeux JP, Thompson ID. 2003. Abnormal functional organization in the dorsal lateral geniculate nucleus of mice lacking the beta 2 subunit of the nicotinic acetylcholine receptor. Neuron 40:1161–1172.

Herrera E, Brown L, Aruga J, Rachel RA, Dolen G, Mikoshiba K, Brown S, Mason CA. 2003. Zic2 patterns binocular vision by specifying the uncrossed retinal projection. Cell 114:545–557.

Hindges R, McLaughlin T, Genoud N, Henkemeyer M, O'Leary DD. 2002. EphB forward signaling controls directional branch extension and arborization required for dorsal-ventral retinotopic mapping. Neuron 35:475–487.

Hornberger MR, Dutting D, Ciossek T, Yamada T, Handwerker C, Lang S, Weth F, Huf J, Wessel R, Logan C, Tanaka H, Drescher U. 1999. Modulation of EphA receptor function by coexpressed ephrinA ligands on retinal ganglion cell axons. Neuron 22:731–742.

Horton JC, Greenwood MM, Hubel DH. 1979. Non-retinotopic arrangement of fibres in cat optic nerve. Nature 282:720–722.

Imondi R, Kaprielian Z. 2001. Commissural axon pathfinding on the contralateral side of the floor plate: a role for B-class ephrins in specifying the dorsoventral position of longitudinally projecting commissural axons. Development 128:4859–4871.

Imondi R, Wideman C, Kaprielian Z. 2000. Complementary expression of transmembrane ephrins and their receptors in the mouse spinal cord: a possible role in constraining the orientation of longitudinally projecting axons. Development 127:1397–1410.

Jeffery G. 2001. Architecture of the optic chiasm and the mechanisms that sculpt its development. Physiol Rev 81:1393–1414.

Kaneko M, Nighorn A. 2003. Interaxonal Eph-ephrin signaling may mediate sorting of olfactory sensory axons in *Manduca sexta*. J Neurosci 23:11523–11538.

Koshiba-Takeuchi K, Takeuchi JK, Matsumoto K, Momose T, Uno K, Hoepker V, Ogura K, Takahashi N, Nakamura H, Yasuda K, Ogura T. 2000. Tbx5 and the retinotectum projection. Science 287:134–137.

Lee JS, Chien CB. 2004. When sugars guide axons: insights from heparan sulphate proteoglycan mutants. Nat Rev Genet 5:923–935.

Lee JS, von der Hardt S, Rusch MA, Stringer SE, Stickney HL, Talbot WS, Geisler R, Nusslein-Volhard C, Selleck SB, Chien CB, Roehl H. 2004. Axon sorting in the optic tract requires HSPG synthesis by ext2 (dackel) and extl3 (boxer). Neuron 44:947–960.

Miller NR, Newman NJ, editors. 1998. Walsh & Hoyt's clinical neuro-ophthalmology, 5th ed. Baltimore: Williams & Wilkins.

Naito J. 1989. Retinogeniculate projection fibers in the monkey optic nerve: a demonstration of the fiber pathways by retrograde axonal transport of WGA-HRP. J Comp Neurol 284:174–186.

Nakagawa S, Brennan C, Johnson KG, Shewan D, Harris WA, Holt CE. 2000. Ephrin-B regulates the ipsilateral routing of retinal axons at the optic chiasm. Neuron 25:599–610.

Pak W, Hindges R, Lim YS, Pfaff SL, O'Leary DD. 2004. Magnitude of binocular vision controlled by islet-2 repression of a genetic program that specifies laterality of retinal axon pathfinding. Cell 119:567–578.

Peters MA. 2002. Patterning the neural retina. Curr Opin Neurobiol 12: 43–48.

Rager U, Rager G, Kabiersch A. 1988. Transformations of the retinal topography along the visual pathway of the chicken. Anat Embryol 179:135–148.

Reese BE, Baker GE. 1993. The re-establishment of the representation of the dorso-ventral retinal axis in the chiasmatic region of the ferret. Vis Neurosci 10:957–968.

Simon DK, O'Leary DD. 1991. Relationship of retinotopic ordering of axons in the optic pathway to the formation of visual maps in central targets. J Comp Neurol 307:393–404.

Simon DK, O'Leary DD. 1992. Influence of position along the medial-lateral axis of the superior colliculus on the topographic targeting and survival of retinal axons. Brain Res Dev Brain Res 69:167–172.

Sperry RW. 1963. Chemoaffinity in the orderly growth of nerve fiber patterns and connections. Proc Natl Acad Sci U S A 50:703–710.

Sperry, RW. 1964. Problems outstanding in the evolution of brain function. James Arthur Lecture. New York: American Museum of Natural History. Reprinted 1977 in: R. Duncan and M. Weston-Smith (Eds.), Enyclopedia of Ignorance, pp. 423–433. Oxford: Pergamon Press.

Thomas JB. 1998. Axon guidance: crossing the midline. Curr Biol 8:R102–104.

Torrealba F, Guillery RW, Eysel U, Polley EH, Mason CA. 1982. Studies of retinal representations within the cat's optic tract. J Comp Neurol 211:377–396.

Walsh C, Guillery RW. 1985. Age-related fiber order in the optic tract of the ferret. J Neurosci 5:3061–3069.

Walsh C, Polley EH, Hickey TL, Guillery RW. 1983. Generation of cat retinal ganglion cells in relation to central pathways. Nature 302:611–614.

Wilkinson DG. 2001. Multiple roles of EPH receptors and ephrins in neural development. Nat Rev Neurosci 2:155–164.

Williams SE, Mann F, Erskine L, Sakurai T, Wei S, Rossi DJ, Gale NW, Holt CE, Mason CA, Henkemeyer M. 2003. Ephrin-B2 and EphB1 mediate retinal axon divergence at the optic chiasm. Neuron 39:919–935.

Yates PA, Roskies AL, McLaughlin T, O'Leary DD. 2001. Topographic-specific axon branching controlled by ephrin-As is the critical event in retinotectal map development. J Neurosci 21:8548–8563.